

## Measurement of four-bond $H^N$ - $H^\alpha$ J-couplings in staphylococcal nuclease

Geerten W. Vuister and Ad Bax

*Laboratory of Chemical Physics, National Institute of Diabetes and Digestive and Kidney Diseases,  
National Institutes of Health, Bethesda, MD 20892, U.S.A.*

Received 27 July 1993

Accepted 5 September 1993

*Keywords:* Four-bond J-coupling; ECOSY; Quantitative J-correlation; Staphylococcal nuclease

---

### SUMMARY

Quantitative J-correlation and triple-resonance ECOSY-type experiments are used to unambiguously establish the presence of four-bond sequential  $H^N$ - $H^\alpha$  J-couplings in the protein staphylococcal nuclease. Substantially negative  ${}^4J_{H^\alpha H^N}$  values, ranging from  $-0.8$  to  $-2.3$  Hz, are observed when the  $\psi$  angle is near  $+120^\circ$ , and the following  $\phi$  angle near  $+60^\circ$ . For other conformations, the four-bond  $H^N$ - $H^\alpha$  J-couplings fall between  $-0.5$  and  $+0.5$  Hz.

---

### INTRODUCTION

The availability of isotopically enriched proteins has stimulated the development of a large number of experiments for the measurement of both homonuclear and heteronuclear J-couplings (Kay et al., 1989; Montelione and Wagner, 1989; Edison et al., 1991; Gemmecker and Fesik, 1991; Schmieder et al., 1991; Wagner et al., 1991; Billeter et al., 1992; Eggenberger et al., 1993). Traditionally, most attention has focused on three-bond couplings because of their well-established dependence on the intervening torsion angle (Bystrov, 1976). One-bond and two-bond J-couplings in proteins also depend on conformation (Delaglio et al., 1991; Mierke et al., 1992; Vuister and Bax, 1992; Vuister et al., 1992), but have not yet been studied extensively.

Four-bond proton-proton coupling constants generally are very small (Bystrov, 1976) and have, to the best of our knowledge, not been observed in peptides or proteins with trans peptide bonds. Below, we report two independent methods for detecting the sequential  $H^\alpha$ - $H^N$  four-bond coupling. The first method is based on the observation of interresidue J-connectivities, using a recently proposed experiment for quantitative J-correlation (Vuister and Bax, 1993). The presence of three unusually large four-bond J-couplings is confirmed and two additional significant J-couplings are found using a 3D triple-resonance experiment based on the ECOSY principle (Griesinger et al., 1986). The size of the  ${}^4J_{H^\alpha H^N}$  couplings shows an unusual angular dependence

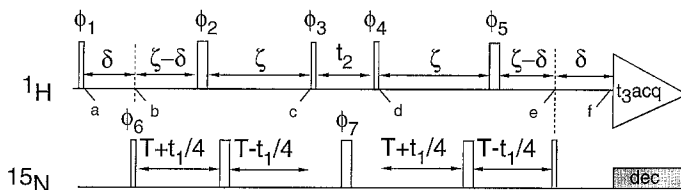


Fig. 1. Pulse scheme of the non-purged 3D HNHA experiment. Narrow and wide pulses, corresponding to  $90^\circ$  and  $180^\circ$  flip angles, respectively, are applied along the x-axis unless indicated otherwise. The following 32-step phase cycle was used:  $\phi_1 = x$ ;  $\phi_2 = 4x, 4(-x), 4(y), 4(-y)$ ;  $\phi_3 = x, -x$ ;  $\phi_4 = 2x, 2(-x)$ ;  $\phi_5 = 4x, 4y, 4(-x), 4(-y)$ ;  $\phi_6 = x$ ;  $\phi_7 = 16x, 16y$ ; receiver =  $4x, 8(-x), 4x, 4(-x), 8x, 4(-x)$ . Quadrature detection in  $t_1$  and  $t_2$  is obtained with the States-TPPI method (Marion et al., 1989b), incrementing phase  $\phi_6$  for  $t_1$  and phases  $\phi_1$ ,  $\phi_2$  and  $\phi_3$  for  $t_2$ . Delays are:  $\delta = 4.5$  ms;  $\zeta = 13.05$  ms. Solvent suppression was achieved by irradiation with a weak RF field ( $\gamma B_2/2\pi \sim 25$  Hz) during the relaxation delay.

in that the largest values occur when  $H_{i-1}^\alpha$ ,  $H_i^N$ , and  $H_i^\alpha$  are approximately in a linear arrangement ( $\psi_{i-1} \approx +120^\circ$ ,  $\phi_i \approx +60^\circ$ ).

## NMR EXPERIMENTS

Figure 1 shows the pulse scheme for the 3D HNHA J-correlation experiment used in the present work. This experiment differs from the original HNHA experiment only by the absence of a  $^1\text{H}$   $90^\circ$  purge pulse immediately prior to data acquisition. A detailed operator formalism description of the original pulse scheme has been presented previously (Vuister and Bax, 1993), and only a brief qualitative description is given below. Magnetization starts on the amide proton and becomes antiphase with respect to its directly attached  $^{15}\text{N}$  at time b. The  $90_{\phi_6}^\circ$  ( $^{15}\text{N}$ ) pulse converts this term into  $^1\text{H}$ - $^{15}\text{N}$  zero- and double-quantum coherences, which are labeled with the  $^{15}\text{N}$  chemical shift by the simultaneous displacement of the first and third  $180^\circ$  ( $^{15}\text{N}$ ) pulses in a constant-time manner. Homonuclear  $\text{H}^N$ - $\text{H}^\alpha$  J-coupling,  $J_{\text{HH}}$ , is active between time points a and c, resulting in a fraction  $\sin(2\pi J_{\text{HH}}\zeta)$  of the  $\text{H}^N$  magnetization that becomes antiphase with respect to  $\text{H}^\alpha$  at time c. The  $90_{\phi_3}^\circ$  ( $^1\text{H}$ ) pulse converts this antiphase  $\text{H}^N$  term into  $\text{H}^\alpha$  magnetization, antiphase with respect to  $\text{H}^N$  in a COSY-type manner, which subsequently is labeled with the  $\text{H}^\alpha$  chemical shift during  $t_2$ . At time c, a fraction  $\cos(2\pi J_{\text{HH}}\zeta)$  of the  $\text{H}^N$  transverse term has not dephased with respect to  $\text{H}^\alpha$  and is not affected by the  $90_{\phi_3}^\circ$  ( $^1\text{H}$ ) pulse. Therefore, this term is labeled during  $t_2$  with its amide proton frequency. The  $90_{\phi_4}^\circ$  ( $^1\text{H}$ ) pulse converts the antiphase  $\text{H}^\alpha$  magnetization back to antiphase  $\text{H}^N$  magnetization without affecting the x component of the in-phase  $\text{H}^N$  magnetization. During the subsequent delay of total duration  $2\zeta$ , a fraction proportional to  $\sin(2\pi J_{\text{HH}}\zeta)$  of the antiphase term rephases to in-phase amide magnetization. At time e the heteronuclear zero- and double-quantum terms are converted back into amide magnetization antiphase with respect to  $^{15}\text{N}$ , which rephases during the final delay  $\delta$ . As shown previously (Vuister and Bax, 1993), application of a  $90^\circ$  ( $^1\text{H}$ ) purge pulse just prior to acquisition results in purely absorptive line shapes in all three dimensions. In the present application the purge pulse is not applied, resulting in higher sensitivity because the antiphase terms present at time f continue to rephase during the detection period  $t_3$ . In the absence of a purge pulse, the line shapes in the 3D spectrum are no longer purely absorptive, and accurate measurement of their integrated intensi-

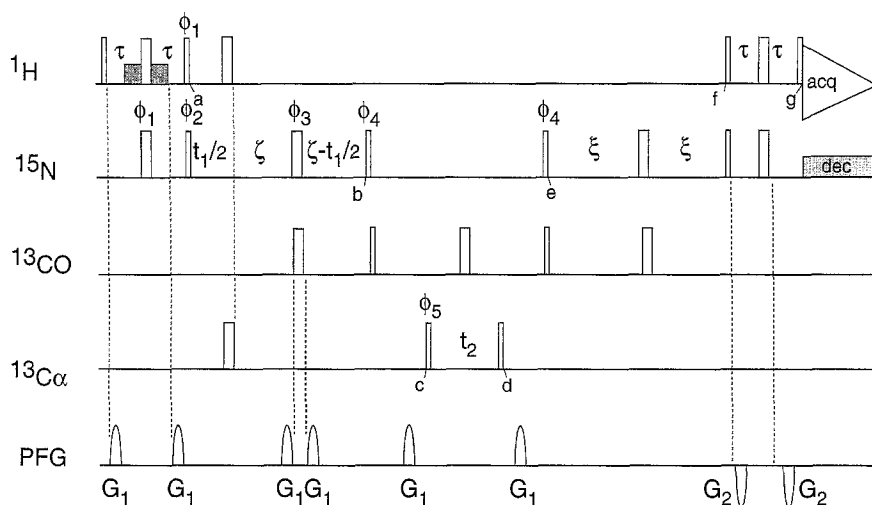


Fig. 2. Pulse scheme for the HN(CO)CA ECOSY experiment. Narrow and wide pulses, corresponding to  $90^\circ$  and  $180^\circ$  flip angles, respectively, are applied along the x-axis unless indicated otherwise. Hatched bars just prior to time point a represent low-power  $90^\circ_{-x}$   $^1\text{H}$  pulses and are part of the solvent-suppression scheme described by Piotto et al. (1992). The following 16-step phase cycle was used:  $\phi_1 = y, -y$ ;  $\phi_2 = x$ ;  $\phi_3 = 4(x), 4(y), 4(-x), 4(-y)$ ;  $\phi_4 = y$ ;  $\phi_5 = 2(x), 2(-x)$ ; receiver =  $x, 2(-x), x, -x, 2(x), -x$ . Quadrature detection in  $t_1$  and  $t_2$  is obtained with the States-TPPI method (Marion et al., 1989b), incrementing phases  $\phi_2$  and  $\phi_5$ , respectively. Pulsed field gradients (PFG) have a sine-bell shape with a strength of 10 G/cm at their maximum and are applied along the z-axis. PFG durations are:  $G_1 = 600 \mu\text{s}$ ;  $G_2 = 600 \mu\text{s}$  (negative polarity). The delay durations are as follows:  $\tau = 2.25 \text{ ms}$ ,  $\zeta = 13.5 \text{ ms}$ , and  $\xi = 10 \text{ ms}$ .

ties becomes difficult. However, the presence of a J-correlation in the non-purged HNHA 3D spectrum indicates the presence of J-coupling, even though exact measurement of its size is not easily accomplished.

The absolute error of a J-coupling measured from an ECOSY-type spectrum is, to first order, not influenced by the magnitude of the J-coupling (Görlach et al., 1993). Therefore, quantitative measurement of very small  $\text{H}_i^\alpha\text{-H}_i^N$  J-couplings can be carried out with an ECOSY version of a constant-time HN(CO)CA experiment (Grzesiek and Bax, 1992) in which care is taken that  $\text{H}^\alpha$  resonances do not change their polarization (Fig. 2). In such an experiment, for every amide proton two correlations to  $\text{C}_{i-1}^\alpha$  are observed, corresponding to  $\text{H}_i^\alpha$  in the  $|\alpha\rangle$  and  $|\beta\rangle$  spin states. These two correlations are displaced from one another by the  $^1\text{J}_{\text{C}^\alpha\text{H}^\alpha}$  splitting in  $F_2$  and by the  $^4\text{J}_{\text{H}^\alpha\text{H}^N}$  splitting in  $F_3$ .

Very briefly, the pulse scheme functions as follows: The initial INEPT scheme transfers magnetization from  $^1\text{H}$  to  $^{15}\text{N}$  and simultaneously suppresses the  $\text{H}_2\text{O}$  resonance using the method proposed by Piotto et al. (1992).  $^{15}\text{N}$  magnetization remains antiphase with respect to the amide proton between time points a and f. Although this choice results in signal loss compared to a scheme in which the nitrogen magnetization would be rephased with respect to its attached  $^1\text{H}$  (Grzesiek and Bax, 1992), it avoids the need for extra  $180^\circ$   $^1\text{H}$  pulses during the remainder of the sequence. Imperfections in such  $180^\circ$  pulses could disrupt the spin state of the  $\text{H}^\alpha$  proton and would result in a partial collapse of the desired ECOSY pattern.  $^{15}\text{N}$  magnetization is chemical-

shift labeled between time points a and b and simultaneously dephases with respect to its adjacent  $^{13}\text{C}$  spin. At time b,  $^{15}\text{N}$  magnetization is transferred to the  $^{13}\text{C}$  spin. Next, the  $^{13}\text{C}$  is correlated with its adjacent  $\text{C}^\alpha$  in an HMQC manner. The large one-bond  $J_{\text{C}^\alpha\text{H}^\alpha}$  coupling is active during  $t_2$  and results in a splitting along the  $F_2$  axis in the 3D spectrum.  $^{13}\text{C}$  magnetization is transferred back to  $^{15}\text{N}$  at time c. During the subsequent  $2\xi$  period, between times e and f,  $^{15}\text{N}$  magnetization rephases with respect to the  $^{13}\text{C}$  prior to an INEPT transfer back to the amide proton. In order to minimize relaxation losses and collapse of the ECOSY pattern resulting from  $\text{H}^\alpha$  spin flips (Görlach et al., 1993), the  $2\xi$  period is kept shorter than the corresponding  $2\zeta$  dephasing period. At time point f, a reverse INEPT scheme transfers magnetization from  $^{15}\text{N}$  back to  $^1\text{H}$  for detection during  $t_3$ . For observation of the desired ECOSY pattern, the  $\text{H}^\alpha$  spin state is kept invariant by the  $90^\circ_x(^1\text{H})-\tau-180^\circ_x(^1\text{H}/^{15}\text{N})-\tau-90^\circ_x(^1\text{H})$  sequence between time points f and g (Madsen et al., 1993).

## EXPERIMENTAL SECTION

Both the HNHA spectrum and the HN(CO)CA ECOSY spectrum were recorded at 35 °C on a Bruker AMX 600 spectrometer. A Bruker triple-resonance probe equipped with a self-shielded z-gradient was used for the HN(CO)CA ECOSY experiment. Sine-bell shaped pulsed field gradients (10 G/cm at the center of the sine bell) were generated with an in-house developed shaping unit and amplifier. The experiments are demonstrated for staphylococcal nuclease (SNase) (1.5 mM in 95%  $\text{H}_2\text{O}/5\%$   $\text{D}_2\text{O}$ ) ligated with  $\text{Ca}^{2+}$  and pdTp. Uniformly  $^{15}\text{N}$ - and  $^{15}\text{N}/^{13}\text{C}$ -labeled protein preparations were used for the HNHA and HN(CO)CA ECOSY experiments, respectively. Data were processed using in-house written software (Delaglio, F., unpublished) and resonance assignments were taken from Baldisseri et al. (1991).

The HNHA spectrum was recorded with the pulse scheme of Fig. 1 as a  $48^* (t_1) \times 48^* (t_2) \times 512^* (t_3)$  dataset ( $n^*$  denotes  $n$  complex data points) with acquisition times of 39.17, 10.56, and 42.00 ms, respectively. The total measuring time, using 128 scans for each hypercomplex  $t_1/t_2$  increment, was 90 h. In the  $t_3$  dimension a solvent-suppression filter was applied to the time-domain data (Marion et al., 1989a), followed by apodization with a  $66^\circ$ -shifted squared sine-bell window, zero-filling to  $1024^*$ , Fourier transformation, and phasing. The data were apodized in  $t_2$  by a  $72^\circ$ -shifted sine-bell window prior to zero-filling to  $256^*$ , Fourier transformation, and phasing. Finally, the duration of the nondecaying  $t_1$  time-domain data was doubled by mirror-image linear prediction (Zhu and Bax, 1990), apodized by a squared cosine-bell window, zero-filled to  $128^*$ , and Fourier transformed. Small baseline distortions in  $F_3$  were removed by an automatic third-order polynomial baseline correction routine.

The HN(CO)CA ECOSY spectrum was recorded with the pulse scheme of Fig. 2 as a  $32^* \times 32^* \times 512^*$  dataset with acquisition times of 24, 10.5, and 55 ms in  $t_1$ ,  $t_2$ , and  $t_3$ , respectively, using 64 scans per  $t_1/t_2$  hypercomplex increment. The residual  $\text{H}_2\text{O}$  resonance was removed by a solvent-suppression filter applied to the  $t_3$  time-domain data (Marion et al., 1989a). Data were apodized by a  $66^\circ$ -shifted squared sine-bell window function and zero-filled to  $2048^*$  in the  $t_3$  domain, prior to Fourier transformation and phasing. In the  $t_1$  and  $t_2$  domains, data were apodized by a  $72^\circ$ -shifted sine-bell window function, zero-filled to  $256^*$ , Fourier transformed, and phased. Peak positions were determined by independent parabolic interpolation in all three dimensions.

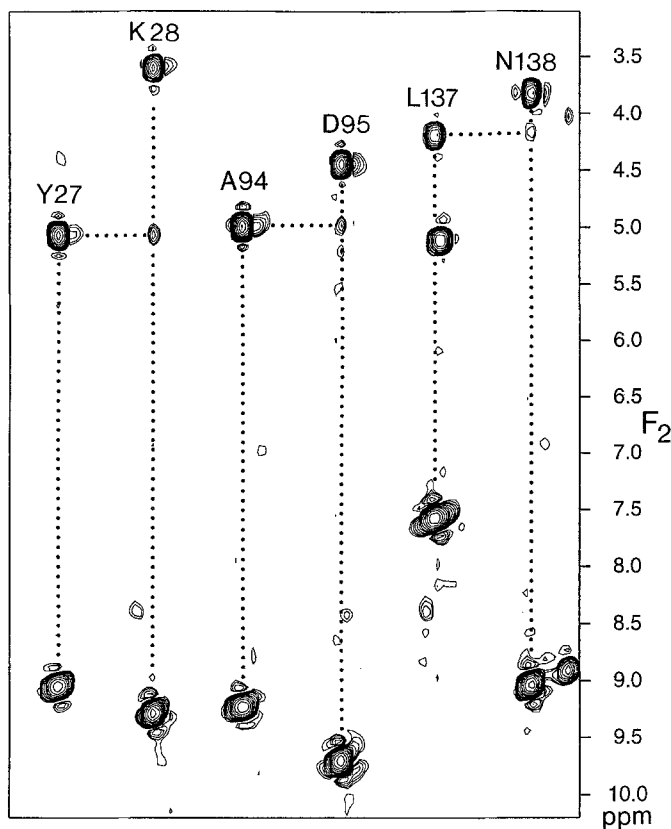


Fig. 3.  $F_2$  strips taken from the non-purged HNHA spectrum of uniformly  $^{15}\text{N}$ -labeled SNase in  $\text{H}_2\text{O}$  at the  $^{15}\text{N}$ - $^1\text{H}$  resonance positions of Tyr<sup>27</sup>, Lys<sup>28</sup>, Ala<sup>94</sup>, Asp<sup>95</sup>, Leu<sup>137</sup>, and Asn<sup>138</sup>. Downfield of  $F_2 = 7$  ppm, only positive contours are drawn, and upfield of 7 ppm, only negative contours.  $F_2$  strips for Lys<sup>28</sup>, Asp<sup>95</sup>, and Asn<sup>138</sup> show sequential  $\text{H}^{\text{N}}$ - $\text{H}^{\alpha}$  correlations, resulting from small  $^4J_{\text{H}^{\alpha}\text{H}^{\text{N}}}$  couplings.

## RESULTS AND DISCUSSION

Figure 3 shows  $F_2$  strips from the non-purged HNHA 3D spectrum of SNase in  $\text{H}_2\text{O}$ , taken at the  $^{15}\text{N}$ - $^1\text{H}$  resonance frequencies of Tyr<sup>27</sup>, Lys<sup>28</sup>, Ala<sup>94</sup>, Asp<sup>95</sup>, Leu<sup>137</sup>, and Asn<sup>138</sup>. Cross peaks resulting from intraresidue  $^3J_{\text{H}^{\alpha}\text{H}^{\text{N}}}$  are observed in the region between 3 and 5.5 ppm for all six residues. Three of the amides (Lys<sup>28</sup>, Asp<sup>95</sup>, and Asn<sup>138</sup>) also show weak four-bond connectivities to the preceding  $\text{H}^{\alpha}$ . A detailed product operator analysis of the HNHA pulse sequence indicates that a J-connectivity to the preceding  $\text{H}^{\alpha}$  can also result from the  $^3J_{\text{NH}^{\alpha}}$  coupling between  $^{15}\text{N}$  and its preceding  $\text{H}^{\alpha}$ . However, this pathway results in dispersive peaks in the  $^{15}\text{N}$  dimension (Vuister and Bax, 1993). As the three four-bond connectivities in Fig. 3 are absorptive in the  $^{15}\text{N}$  dimension of the 3D spectrum, they cannot be the result of  $^3J_{\text{NH}^{\alpha}}$  coupling. Four-bond  $\text{H}^{\text{N}}$ - $\text{H}^{\alpha}$  J-couplings of appreciable size previously have been reported only for cis peptide bonds (Aubry et al., 1974), whereas on the basis of finite perturbation calculations values for trans peptide bonds are expected to be very small ( $< 0.5$  Hz) (Bystrov, 1976). However, Lys<sup>28</sup>, Asp<sup>95</sup>, and Asn<sup>138</sup> all are preceded by trans peptide bonds and constitute the second residue in type I' and type II' reverse

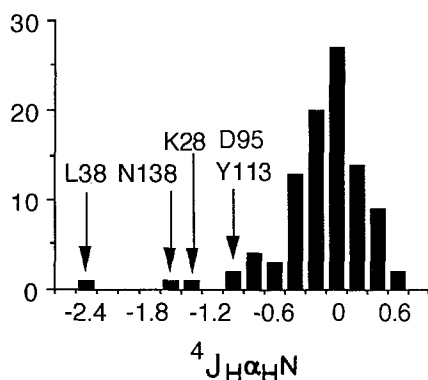


Fig. 4. Histogram of the  ${}^4J_{\text{H}^\alpha\text{H}^\text{N}}$  couplings in SNase as measured from the HN(CO)CA ECOSY spectrum.

turns (Loll and Lattman, 1989), with positive  $\phi$  angles near  $60^\circ$ . The first residue in each of the three turns has a  $\psi$  angle between  $118^\circ$  and  $135^\circ$ . This conformation results in a linear arrangement of the amide proton, its intraresidue  $\text{H}^\alpha$ , and its preceding  $\text{H}^\alpha$ , with very short distances ( $\sim 2.1 \text{ \AA}$ ) between  $\text{H}^\text{N}$  and the two  $\text{H}^\alpha$  protons.

In principle, this type of geometry can give rise to coherence transfer between  $\text{H}_i^{\alpha-1}$  and  $\text{H}_i^\text{N}$  via a cross-correlation relaxation mechanism (Wimperis and Bodenhausen, 1989): The dipolar local fields from the two  $\text{H}^\alpha$  spins at the  $\text{H}^\text{N}$  position nearly cancel one another if the two  $\text{H}^\alpha$  nuclei have opposite spin states, but reinforce one another if both are in the same spin state. Numerical calculations for a linear arrangement of the  $\text{H}_{i-1}^\alpha$ ,  $\text{H}_i^\text{N}$ , and  $\text{H}_i^\alpha$  spins at  $2.1 \text{ \AA}$  distance, using a rotational correlation time  $\tau_c$  of 9 ns, indicate that the contribution of a cross-correlation mechanism gives rise to an amount of coherence transfer that is comparable to that of a direct  ${}^4J_{\text{H}^\alpha\text{H}^\text{N}}$  of only ca. 0.2 Hz. Intensities of the cross peaks in Fig. 3 are indicative of  ${}^4J_{\text{H}^\alpha\text{H}^\text{N}}$  in the 1–2 Hz range.

Measurement of J-couplings in an ECOSY-type spectrum is not influenced by this cross-correlation effect and is therefore used to evaluate the presence of four-bond J-couplings in an independent way. Ninety  ${}^4J_{\text{H}^\alpha\text{H}^\text{N}}$  couplings were measured for well-separated  $\text{C}_{i-1}^\alpha\text{-N}_i\text{-H}_i^\text{N}$  correlations in the 3D HN(CO)CA ECOSY spectrum and are shown as a histogram in Fig. 4. Clearly, the values are very small and cluster around zero Hz. Restricting the measurement to 21 amides in  $\alpha$ -helices, which are all expected to have very similar  ${}^4J_{\text{H}^\alpha\text{H}^\text{N}}$  values, an average of  $+0.10 \text{ Hz}$  is obtained with an rmsd of  $0.17 \text{ Hz}$ . Not accounting for systematic errors that may be induced by relaxation (Görlach et al., 1993; Harbison, 1993), the precision of the present measurement is, therefore, approximately  $0.2 \text{ Hz}$ . The five most negative  ${}^4J_{\text{H}^\alpha\text{H}^\text{N}}$  values in the histogram of Fig. 4 correspond to couplings to the amides of Lys<sup>28</sup>, Leu<sup>38</sup>, Asp<sup>95</sup>, Tyr<sup>113</sup>, and Asn<sup>138</sup>, and the corresponding ECOSY patterns are displayed in Fig. 5. Each correlation is split in the  $F_2$  domain by the large  ${}^1J_{\text{C}^\alpha\text{H}^\alpha}$  coupling and for all five correlations small  ${}^4J_{\text{H}^\alpha\text{H}^\text{N}}$  displacements are observed in the  $F_3$  dimension. The  $F_2$  and  $F_3$  displacements are opposite in sign, indicating that  ${}^4J_{\text{H}^\alpha\text{H}^\text{N}}$  is negative when assuming a positive value for  ${}^1J_{\text{C}^\alpha\text{H}^\alpha}$ . Values measured for Tyr<sup>27</sup>-Lys<sup>28</sup>, Leu<sup>37</sup>-Leu<sup>38</sup>, Ala<sup>94</sup>-Asp<sup>95</sup>, Ala<sup>112</sup>-Tyr<sup>113</sup>, and Leu<sup>137</sup>-Asn<sup>138</sup> are  $-1.3$ ,  $-2.3$ ,  $-1.0$ ,  $-0.8$ , and  $-1.5 \text{ Hz}$ , respectively. The  ${}^4J_{\text{H}^\alpha\text{H}^\text{N}}$  coupling for Ala<sup>112</sup>-Tyr<sup>113</sup> is too small to yield an observable cross-peak intensity in the HNHA spectrum, whereas the  ${}^4J_{\text{H}^\alpha\text{H}^\text{N}}$  coupling for Leu<sup>38</sup> could not be observed in the HNHA spectrum due to overlap of the  $\text{H}^\alpha$  resonances of Leu<sup>37</sup> and Leu<sup>38</sup>.

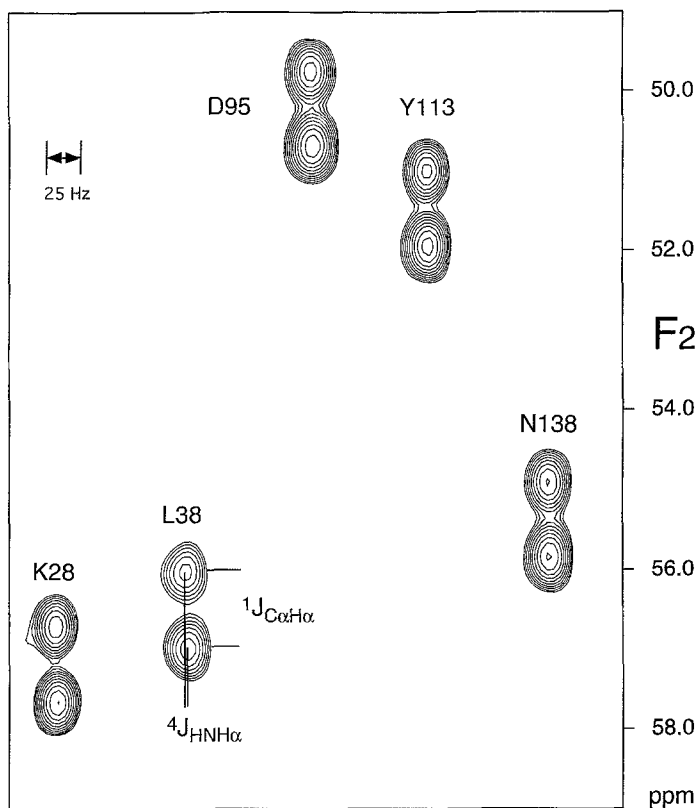


Fig. 5.  $F_2$  strips taken from the HN(CO)CA ECOSY spectrum of uniformly  $^{15}\text{N}/^{13}\text{C}$ -labeled SNase in  $\text{H}_2\text{O}$  taken at the  $^{15}\text{N}$ - $^1\text{H}$  resonance positions of Lys<sup>28</sup>, Leu<sup>38</sup>, Asp<sup>95</sup>, Tyr<sup>113</sup>, and Asn<sup>138</sup>. Splitting along the  $F_2$ -axis results from the large  $^1J_{\text{C}\alpha\text{H}\alpha}$  coupling and displacement along the  $F_3$ -axis results from  $^4J_{\text{H}\alpha\text{H}\text{N}}$  couplings.

Previous work on four-bond couplings showed a strong dependence of the four-bond  $^4J_{\text{FH}\alpha}$  coupling in *N*-fluoroamide derivatives on the intervening N-C $^\alpha$ -CO-N torsion angle,  $\psi$ , with the largest absolute value (ca. 23 Hz) at a dihedral angle, H $^\alpha$ -C $^\alpha$ -C-O, of 180°, i.e.,  $\psi = 120^\circ$  (Hammer and Chandrasegaran, 1984). FPT-INDO calculations by Barfield et al. (1975) for propane also suggest a maximum negative value for an arrangement where the two coupled protons are most proximate, but their results for propene are substantially different. Neither study suggests any dependence of the four-bond J-coupling on the non-intervening bond angle  $\phi$  and our results are therefore quite surprising.

## CONCLUSIONS

The two conceptually different experiments described above show the presence of significant  $^4J_{\text{H}\alpha\text{H}\text{N}}$  couplings for five dipeptide segments in SNase with  $\psi$  angles near  $+120^\circ$  and  $\phi$  angles near  $+60^\circ$ . For all five segments the sign of the  $^4J_{\text{H}\alpha\text{H}\text{N}}$  coupling constant is found to be negative, assuming a positive value for  $^1J_{\text{C}\alpha\text{H}\alpha}$ . The values measured for the five  $^4J_{\text{H}\alpha\text{H}\text{N}}$  coupling constants are much larger than expected for residues with trans peptide bonds and show an unexpected

correlation with the  $\phi$  angle. The fact that the four-bond J-couplings for the  $\alpha$ -helical residues in SNase are very similar to one another, with an rmsd of only 0.17 Hz, indicates that the precision of the J-coupling measurement is at least 0.2 Hz. This is highly remarkable, considering that a  $t_3$  acquisition time of only 55 ms was used. Apparently, the pulsed field gradients have eliminated the residual small phase distortions that sometimes plague ECOSY-type measurements and, combined with the high signal-to-noise ratio obtained for the  $H^N$ - $C^\alpha$  correlation, this results in very precise measurement of the J-coupling.

## ACKNOWLEDGEMENTS

We thank Dennis Torchia for providing the SNase sample, Rolf Tschudin for technical support, Michael Barfield (University of Arizona) for valuable discussions and Andy Wang for useful comments during the preparation of the manuscript. This work was supported by the AIDS Targeted Anti-Viral Program of the Office of the Director of the National Institutes of Health.

## REFERENCES

- Aubrey, A., Giessner-Prettre, C., Cung, M.T., Marraud, M. and Neel, J. (1974) *Biopolymers*, **13**, 523–531.
- Baldisseri, D.M., Torchia, D.A., Poole, L.B. and Gerlt, J. (1991) *Biochemistry*, **30**, 3628–3633.
- Barfield, M., Dean, A.M., Fallick, C.J., Spear, R.J., Sternell, S. and Westerman, P.W. (1975) *J. Am. Chem. Soc.*, **97**, 1482–1492.
- Billeter, M., Neri, D., Otting, G., Qian, Y.Q. and Wüthrich, K. (1992) *J. Biomol. NMR*, **2**, 257–274.
- Bystrov, V.F. (1976) *Prog. NMR Spectrosc.*, **10**, 41–81.
- Delaglio, F., Torchia, D. and Bax, A. (1991) *J. Biomol. NMR*, **1**, 439–446.
- Edison, A.S., Westler, W.M. and Markley, J. (1991) *J. Magn. Reson.*, **92**, 434–438.
- Eggenberger, U., Karimi-Nejad, Y., Thüring, H., Rüterjans, H. and Griesinger, C. (1993) *J. Biomol. NMR*, **2**, 583–590.
- Gemmecker, G. and Fesik, S.W. (1991) *J. Magn. Reson.*, **95**, 208–213.
- Görlach, M., Wittekind, M., Farmer II, B.T., Kay, L.E. and Mueller, L. (1993) *J. Magn. Reson. Ser. B*, **101**, 194–197.
- Griesinger, C., Sørensen, O.W. and Ernst, R.R. (1986) *J. Chem. Phys.*, **85**, 6837–6843.
- Grzesiek, S. and Bax, A. (1992) *J. Magn. Reson.*, **96**, 432–440.
- Hammer, C.F. and Chandrasegaran, S. (1984) *J. Am. Chem. Soc.*, **106**, 1543–1552.
- Harbison, G. (1993) *J. Am. Chem. Soc.*, **115**, 3026–3027.
- Kay, L.E., Brooks, B., Sparks, S.W., Torchia, D.A. and Bax, A. (1989) *J. Am. Chem. Soc.*, **111**, 5488–5490.
- Loll, P.J. and Lattman, E.E. (1989) *Protein Struct. Funct. Genet.*, **5**, 183–201.
- Madsen, J.G., Sørensen, O.W., Sørensen, P. and Poulsen, F.M. (1993) *J. Biomol. NMR*, **3**, 239–244.
- Marion, D., Ikura, M. and Bax, A. (1989a) *J. Magn. Reson.*, **84**, 425–430.
- Marion, D., Ikura, M., Tschudin, R. and Bax, A. (1989b) *J. Magn. Reson.*, **85**, 393–399.
- Mierke, D.F., Grdadolnik, S.G. and Kessler, H. (1992) *J. Am. Chem. Soc.*, **114**, 8283–8284.
- Montelione, G. and Wagner, G. (1990) *J. Magn. Reson.*, **87**, 183–188.
- Piotto, M., Saudek, V. and Sklenar, V. (1992) *J. Biomol. NMR*, **2**, 661–666.
- Schmieder, P., Kurz, M. and Kessler, H. (1991) *J. Biomol. NMR*, **1**, 403–420.
- Vuister, G.W. and Bax, A. (1992) *J. Biomol. NMR*, **2**, 401–405.
- Vuister, G.W. and Bax, A. (1993) *J. Am. Chem. Soc.*, **115**, 7772–7777.
- Vuister, G.W., Delaglio, F. and Bax, A. (1992) *J. Am. Chem. Soc.*, **114**, 9674–9675.
- Wagner, G., Schmieder, P. and Thanabal, V. (1991) *J. Magn. Reson.*, **93**, 436–440.
- Wimperis, S. and Bodenhausen, G. (1989) *Mol. Phys.*, **66**, 897–919.
- Zhu, G. and Bax, A. (1990) *J. Magn. Reson.*, **90**, 405–410.